

# Sol–Gel Synthesis of Low-Loss MgTiO<sub>3</sub> Thin Films by a Non-Methoxyethanol Route

Kuzhichalil P. Surendran,<sup>†</sup> Aiying Wu,<sup>†</sup> Paula M. Vilarinho,<sup>\*,†</sup> and Victor M. Ferreira<sup>‡</sup>

Department of Ceramics and Glass Engineering and Department of Civil Engineering, CICECO, University of Aveiro, 3810-193 Aveiro, Portugal

Received October 28, 2007. Revised Manuscript Received April 11, 2008

A cost-effective and hazard-free sol–gel method for the synthesis of single-phase MgTiO<sub>3</sub> thin film is reported here, using (MgNO<sub>3</sub>)<sub>2</sub>·6H<sub>2</sub>O and TiC<sub>16</sub>H<sub>36</sub>O<sub>4</sub> as precursors and employing either acetic acid or acetyl acetone as the stabilizers for titanium n-butoxide. The effect of the stabilizers on the structure, microstructure and electrical properties is evaluated. Acetyl-acetone-based films have a denser and more homogeneous microstructure than the acetic-acid-derived films, which is directly reflected in their dielectric properties. Acetyl acetone derived films annealed at 700 °C exhibit a dielectric constant,  $\epsilon_r = 16.3$  and dielectric loss,  $\tan \delta = 0.0021$  at 1 MHz. The differences are attributed to the lower reactivity of acetyl-acetone-stabilized sols and higher crystallization temperature of acetyl acetone derived films.

## 1. Introduction

Over the last two decades, the global telecommunication industry is growing toward faster, thinner, and lighter technologies, which has culminated in the development of novel 4G mobile technology.<sup>1</sup> In mobile phones, global positioning systems (GPS), and satellite communications, the demand for monolithic microwave integrated circuit technologies (MMIC) utilizing low-loss dielectrics has been exponentially increasing. Ilmenite structured MgTiO<sub>3</sub> is a promising low-loss dielectric<sup>2</sup> with high quality factor ( $Q$  above 20 000 at 8 GHz) and intermediate dielectric constant ( $\epsilon_r = 17$ ), but with a negative temperature coefficient of resonant frequency ( $\tau_f = -50$  ppm/°C) which could be tailored to zero using suitable doping.<sup>3</sup> This dielectric is widely used in many microwave applications like transverse electromagnetic mode quarter wave resonators,<sup>4</sup> band-pass filters,<sup>5</sup> 90° hybrid couplers,<sup>6</sup> multilayer capacitors,<sup>7</sup> and so forth. Apart from its microwave resonator applications, magnesium metatitanate could also be used for optical communication in planar lightwave circuits (PLC) as a buffer layer for sapphire and LiNbO<sub>3</sub>.<sup>8</sup> However, most of the studies on pure and doped MgTiO<sub>3</sub> dielectrics are limited to its bulk ceramic form and there is a surprising scarcity of literature on thin film characteristics of MgTiO<sub>3</sub>.

Despite the technological interest of this material, obtaining phase purity in MgTiO<sub>3</sub> is difficult both in solid state and solution methods because of its narrow range of phase stability. The sol–gel process has been frequently used in thin film technology for different microelectronic systems, because of its versatility as an effective technique to fabricate high-quality dielectric and ferroelectric films. This methodology possesses many advantages including low processing temperature, together with high purity and homogeneity of the product. The synthesis of pure phase MgTiO<sub>3</sub> using sol–gel methods was greatly constrained by the formation of additional phases. The low solubility of magnesium alkoxides is believed as the primary impediment for sol–gel synthesis of this complex oxide, which has to be addressed by suitable modifications at the precursor level.<sup>9</sup> In a recent report on sol–gel synthesis of MgTiO<sub>3</sub> powders by Miao et al.,<sup>10</sup> impurity phases like MgTi<sub>2</sub>O<sub>5</sub> and Mg<sub>2</sub>TiO<sub>4</sub> appeared up to 600 °C disappearing at 700 °C, with the appearance of extra TiO<sub>2</sub>, consequent to the decomposition of the former. But from a thin film technology perspective, only very few reports are available. Using a modified sol–gel method, Choi and Lee<sup>11</sup> fabricated MgTiO<sub>3</sub> thin films. However, their objective was to test the adaptability of MgTiO<sub>3</sub> as a cladding layer to LiNbO<sub>3</sub> and silica, in thin film optical waveguide. In the recent past, MgTiO<sub>3</sub> thin films were prepared by rf-sputtering, but the observed high dissipation factor (0.041 at 10 MHz),<sup>12</sup> which obviously hinders the practical application of these films, demands several modifications in the fabrication process.

For the synthesis of MgTiO<sub>3</sub> powders by sol–gel processing, the most frequently used methodology is the one that involves 2-methoxyethanol (2-MOE), because of the ability

\* Corresponding Author: paula.vilarinho@ua.pt.

<sup>†</sup> Department of Ceramics and Glass Engineering, CICECO, University of Aveiro.

<sup>‡</sup> Department of Civil Engineering, CICECO, University of Aveiro.

- (1) Gow, G. A.; Smith, R. K. *Mobile and Wireless Communications: An Introduction* Open University Press: Berkshire, U.K., 2006.
- (2) Wakino, K. *Ferroelectrics* **1989**, *91*, 69.
- (3) Ferreira, V. M.; Baptista, J. L. *Mater. Res. Bull.* **1994**, *29*, 1017.
- (4) Wakino, K.; Nishikawa, T.; Ishikawa, Y.; Matsumoto, H. *IEEE IT-S Cat. No. 81CH1592-5*. **1981**, 185.
- (5) Huang, C.-L.; Tsai, C.-M.; Yang, A.; Hsu, A. *Microwave Opt. Lett.* **2005**, *44*, 421.
- (6) Tanaka, H.; Banba, N.; Arai, S.; Nishikawa, T. *IEEE MTT-S Digest* **1994**, 903.
- (7) Bernard, J.; Houivet, D.; El Fallah, J.; Haussonne, J. M. *J. Eur. Ceram. Soc.* **2004**, *4*, 1877.
- (8) Choi, Y. H.; Lee, J. *Thin Solid Films* **2001**, *385*, 43.

(9) Abothu, I. R.; Rao, A.V. P.; Komarneni, S. *Mater. Lett.* **1999**, *38*, 186.

(10) Miao, Y.-M.; Zhang, Q.-L.; Yang, H.; Wang, H.-P. *Mater. Sci. Eng., B* **2006**, *128*, 103.

(11) Lee, J.; Choi, C. W. *Jpn. J. Appl. Phys.* **1999**, *38*, 3651.

(12) Huang, C.-L.; Chen, Y.-B. *Jpn. J. Appl. Phys.* **2005**, *44*, 6736.

of this solvent to solubilize a variety of starting reagents.<sup>13</sup> However, 2-MOE is a known teratogen, which presents a safety concern and inhibits its use in most manufacturing facilities.<sup>14</sup> Besides, the 2-MOE-based process is time-consuming, involving repeated distillation and refluxing strategies; the procedure sophistication can be overwhelming<sup>21</sup> from a technological perspective as well. An efficient way of avoiding the use of 2-MOE is to react the Ti-alkoxide with a suitable coordinating agent like acetic acid (HOAc) or acetyl acetone (AcAc).<sup>14</sup> Compared to the complex 2-MOE route, these processes offer the advantages of relative simplicity of the synthesis, and moreover, the involved distillation and refluxing strategies are not required. In the synthesis of low-loss materials like MgTiO<sub>3</sub>, a major challenge is the control of the hydrolysis of titanium precursor, which subsequently affects the stability of the sol and of the crystalline phase. In addition, several other factors are also to be considered, such as the solubility of Mg-containing species, reactivity between the precursor reagents, decomposition pathway, and microstructural evolution behavior. All of these parameters control to a great extent the film quality, which in turn controls the dielectric losses.

A detailed investigation on the sol–gel synthesis of MgTiO<sub>3</sub> thin films by a non-MOE route using two different coordinating agents for titanium butoxide is conducted in this work. The aging of the sols, pyrolysis, crystallization, and morphology of the films prepared using the two methodologies are compared and related to the final dielectric properties of MgTiO<sub>3</sub> films.

## 2. Experimental Section

Magnesium nitrate, (Mg(NO<sub>3</sub>)<sub>2</sub>·6H<sub>2</sub>O (Merck, 99%), and titanium butoxide, TiC<sub>16</sub>H<sub>36</sub>O<sub>4</sub> (Merck 98%), were used as the starting materials for the sol–gel synthesis of MgTiO<sub>3</sub> films. A stoichiometric amount of magnesium nitrate was dissolved in ethanol, CH<sub>3</sub>CH<sub>2</sub>OH (Panreac Quimica, 99.5%), and refluxed at 60 °C under constant stirring for 2 h. The magnesium salt to ethanol solvent molar ratio was maintained as 1:10. 1,2-Propanediol (Aldrich, 99.5%) was added to this homogenized mixture, as a surface modifier, which was again stirred thoroughly for 1 h at room temperature. The titanium precursor was prepared in two different ways: in the first case, titanium butoxide was stabilized using glacial acetic acid, C<sub>2</sub>H<sub>4</sub>O<sub>2</sub> (Aldrich, 99.8%), whereas acetyl acetone (Aldrich, 99.5%) was used as the coordinating agent in the second one. An equimolar ratio is maintained between the coordinating agent and 1,2-propanediol. However, the coordinating agent to the titanium precursor molar ratio is optimized at 2. The stabilized titanium precursor and magnesium solution were mixed at a molar ratio of 1:1. Finally, ethanol was used to dilute the solution to 0.1 M. The sols derived from both routes were kept in demoinsturized conditions for 1–6 months to study the effects of aging. Thin films were prepared by spin-coating using freshly prepared sols at 4000 rpm for 30 s on a cleaned platinum-coated silicon substrates (Pt/TiO<sub>2</sub>/SiO<sub>2</sub>/ (100)Si). The water needed for polycondensation is automatically provided by the moisture from the atmosphere at the time of spin coating. The spin-coated films were heat-treated at 200 °C for 5 min and subsequently pyrolyzed at 300 °C in the case of acetic

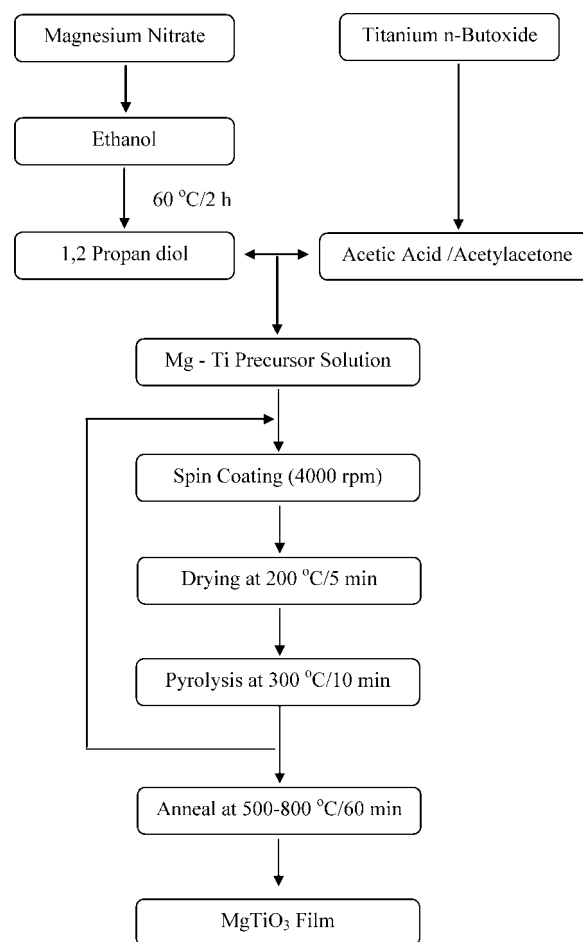


**Figure 1.** Schematic representation of the major experimental steps involved in the preparation of MgTiO<sub>3</sub>.

acid and at 350 °C in the case of acetyl-acetone-derived films, for 10 min for each deposited layer. This cycle was repeated in order to get films with a final thickness around 550 nm. The films were annealed for 1 h at different temperatures from 500 to 800 °C in air atmosphere. The flowchart for the synthesis of MgTiO<sub>3</sub> films is summarized in Figure 1.

The stability of MgTiO<sub>3</sub> precursor sols was analyzed by measuring their rheological behavior using a cone and plate viscometer (Carri-med, CSL500). The phase-evolution analysis was conducted by thermogravimetric-differential thermal analysis (Lab-sys Setaram TG-DTA/DSC, Caluire, France) with a heating rate of 20 °C/min in air, and X-ray diffraction analysis (XRD, Rigaku, D/Max-B). The thermal analysis was carried out with dried powders obtained by drying the precursor solution at 80 °C for 2 days. The morphology and thickness of MgTiO<sub>3</sub> films were evaluated by scanning electron microscopy (SEM, Hitachi, S-4100). The surface analysis of MgTiO<sub>3</sub> films delivered from two routes was also carried out using atomic force microscopy (AFM) in tapping mode. A commercial AFM (Picoscan 2500, Molecular Imaging, Agilent Technology) was used in the current experiment. A silicon cantilever (type: ACT, Scientec) was employed to acquire topographic and phase images of the film surface simultaneously.

For electrical characterization, Au electrodes ( $\varnothing \approx 0.6$  mm) were sputtered on the surface of the films using a shadow mask to form metal–insulator–metal (MIM) capacitors. The dielectric permittivity and loss factor were measured at different frequencies between 100 Hz and 1 MHz at room temperature, using a Hewlett-Packard LCR meter (HP 4284A) impedance/gain analyzer. The electroded films were annealed at 200 °C for 15 min to improve the interfaces

(13) Lee, B. D.; Yoon, K. H.; Kim, E. S.; Kim, T. H. *Jpn. J. Appl. Phys.* **2003**, *42*, 6158.

(14) Schwartz, R. W. *Chem. Mater.* **1997**, *9*, 2325.

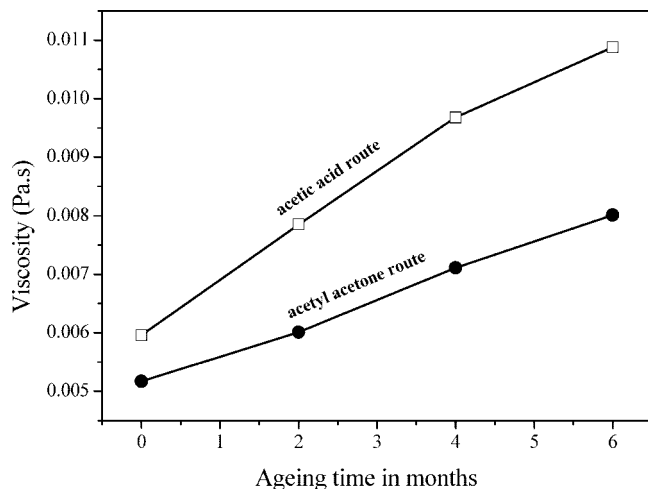


**Figure 2.** Variation of viscosity of sols with aging.

between the metal and the film, before the dielectric measurements were performed.

### 3. Results

Figure 2 shows the variation of viscosity as a function of aging time for the two different sols. The viscosities of the freshly prepared sols are comparable; 0.00596 Pa s for the acetic-acid-based sols, and 0.00517 Pa s for the acetyl-acetone-based ones. As aging time increases, the viscosities of both sols increased but with different rates, as indicated by the slope of the plots. After the solution was aged for 6 months, the viscosity variation for acetyl acetone precursor sol is only 55%, whereas that for acetic acid counterpart is 82%, as given in Figure 2. Furthermore, this study revealed that the shelf life of acetic-acid-based sol is only about 10 months, precipitating afterward. The higher viscosity variation and subsequent precipitation of acetate precursor might be attributed to the continuous condensation reactions and agglomeration of polymeric species resulted from the faster hydrolysis rates.<sup>15</sup>

Figure 3a represents the DTA profiles of the dried  $\text{MgTiO}_3$  gels derived from acetyl-acetone- and acetic-acid-based precursors. The endothermic peaks around 160 °C for acetic-acid-based sol, and 170 °C for acetyl-acetone-based sol, are due to the elimination of physisorbed water. During the thermal evolution of magnesium metatitanate gels, the major process involved is the combustion of the organic matter, mainly carboxylic groups that starts around 180 °C in acetic acid sols and 190 °C in acetyl-acetone-based sols, respectively. The onset of crystallization of  $\text{MgTiO}_3$  takes place above 450 °C in acetyl acetone route as indicated by the exothermic peak around 475 °C. On the other hand, in the acetic-acid-derived sample the crystallization of the desired magnesium metatitanate appeared as a diffuse exothermic reaction, which happens at slightly lower temperature (<450 °C). However, at higher temperatures,  $\text{MgTiO}_3$  starts to decompose into  $\text{Mg}_2\text{TiO}_4$  and rutile (i.e.,  $2\text{MgTiO}_3 \rightarrow \text{Mg}_2\text{TiO}_4 + \text{TiO}_2$ ), which appeared as exothermic peaks around 727 and 757 °C in acetic-acid- and acetyl-acetone-

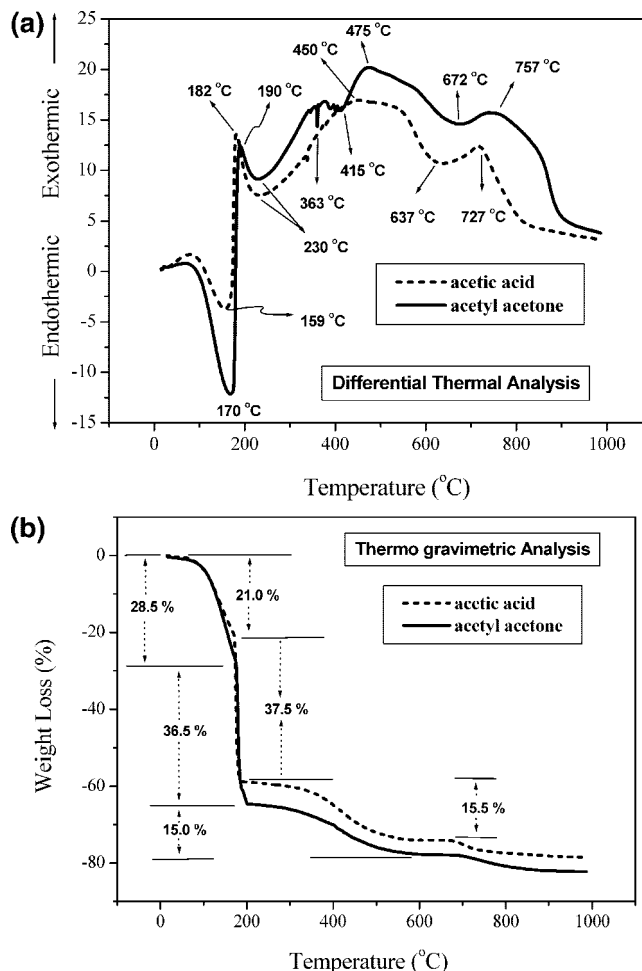


**Figure 3.** (a) DTA profile of the dried sols prepared using acetic acid and acetyl acetone chelates. (b) Thermogravimetric profiles of the dried sols prepared using acetic acid and acetyl acetone chelates.

based gels, respectively. Figure 3b represents the thermogravimetric analysis (TG) plots of dried  $\text{MgTiO}_3$  gels derived from acetyl acetone and acetic acid. It is evident that the total weight loss of the acetyl acetone derived gel is higher than that of acetic acid. The weight loss corresponding to the dehydroxylation of the sols is 21% in acetic-acid-based sols, whereas it is 28.5% in acetyl acetone counterpart. In both gels, the burning of organic matter is accompanied by the greatest weight loss (>35%), which occurs between 200 and 400 °C.

It is a well-known fact that the crystallization mechanism of magnesium metatitanate is complex,<sup>3</sup> and X-ray diffraction analysis of the dried sols calcined at different temperatures could reveal the narrow temperature range where crystallinity and phase stability of  $\text{MgTiO}_3$  is optimum. The evolution of  $\text{MgTiO}_3$  phase from amorphous sols was studied by heating the dried gels at various temperatures (from 400 to 750 °C in case of acetic-acid-based gels and from 400 to 775 °C in the case of acetyl acetone ones) and the corresponding powder diffraction patterns are shown in patterns a and b in Figure 4. In acetic-acid-based sols, crystallization of  $\text{MgTiO}_3$  (JCPDS File Card No. 06-0494) starts at 440 °C in accordance with the DTA information. At this temperature, additional phases of  $\text{MgTi}_2\text{O}_5$  (JCPDS File Card No. 35-0792) and  $\text{TiO}_2$  (JCPDS File Card No.

(15) Gonzalez, M. B.; Wu, A.; Vilarinho, P. M. *Chem. Mater.* **2006**, *18*, 1737.

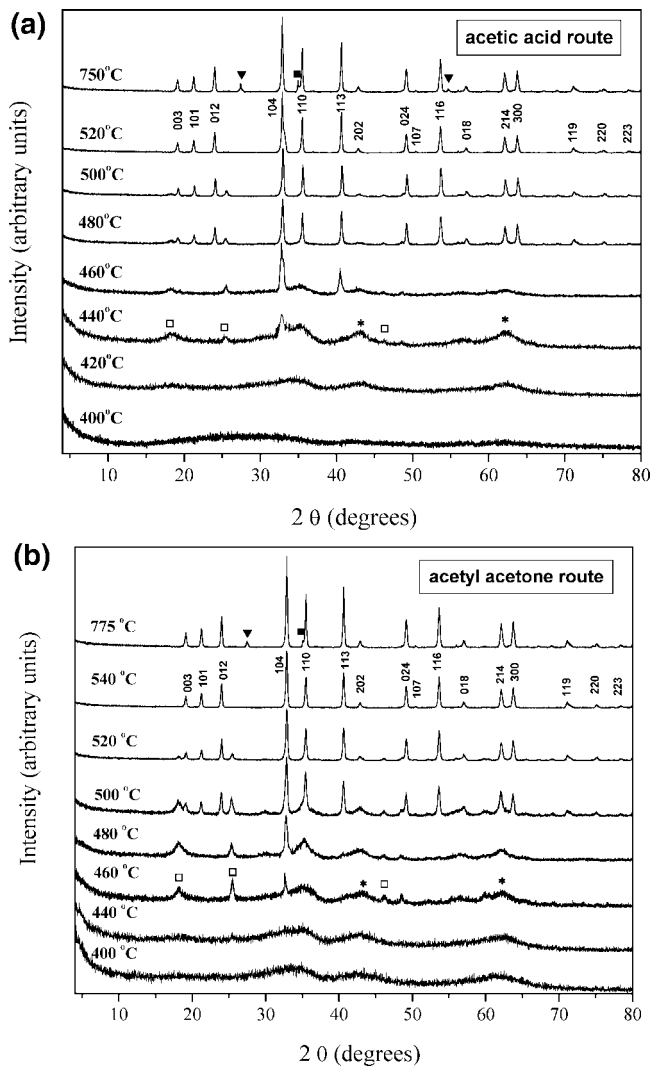


**Figure 4.** (a) XRD patterns of dried sol derived from acetic acid route as a function of calcination temperature ( $\square$  represents  $\text{MgTi}_2\text{O}_5$ , \* represents  $\text{TiO}$ ,  $\blacksquare$  represents  $\text{Mg}_2\text{TiO}_4$ , and  $\blacktriangledown$  represents rutile). (b) XRD patterns of dried sol derived from acetyl acetone route as a function of calcination temperature ( $\square$  represents  $\text{MgTi}_2\text{O}_5$ , \* represents  $\text{TiO}$ ,  $\blacksquare$  represents  $\text{Mg}_2\text{TiO}_4$ , and  $\blacktriangledown$  represents rutile).

09–0240) are also present. Pure  $\text{MgTiO}_3$  is achieved in this route at 520 °C. This formation temperature is considerably lower than the temperature reported (620 °C) in recent works for  $\text{MgTiO}_3$  powder synthesis through the sol–gel technique.<sup>16</sup> On the other hand, in acetyl-acetone-derived sols, besides the  $\text{MgTi}_2\text{O}_5$  phase, trace amounts of  $\text{TiO}_2$  are detected at calcination temperatures between 420 and 440 °C. As the calcination temperature reaches 460 °C, the crystallization of  $\text{MgTiO}_3$  starts. In this case, the pure  $\text{MgTiO}_3$  phase could be synthesized only at a slightly higher temperature ( $\sim 540$  °C) compared to acetic-acid-based sols. As evidenced by an exothermic peak in thermal analysis, the acetic-acid-derived gel exhibited signs of decomposition when calcined at 750 °C and the presence of  $\text{Mg}_2\text{TiO}_4$  (JCPDS File Card No. 25–1157) and  $\text{TiO}_2$  (JCPDS File Card No. 21–1276) were detected. In the case of acetyl-acetone-based gel, the decomposition is occurring at a slightly higher temperature ( $\sim 775$  °C) (see Figure 4b).

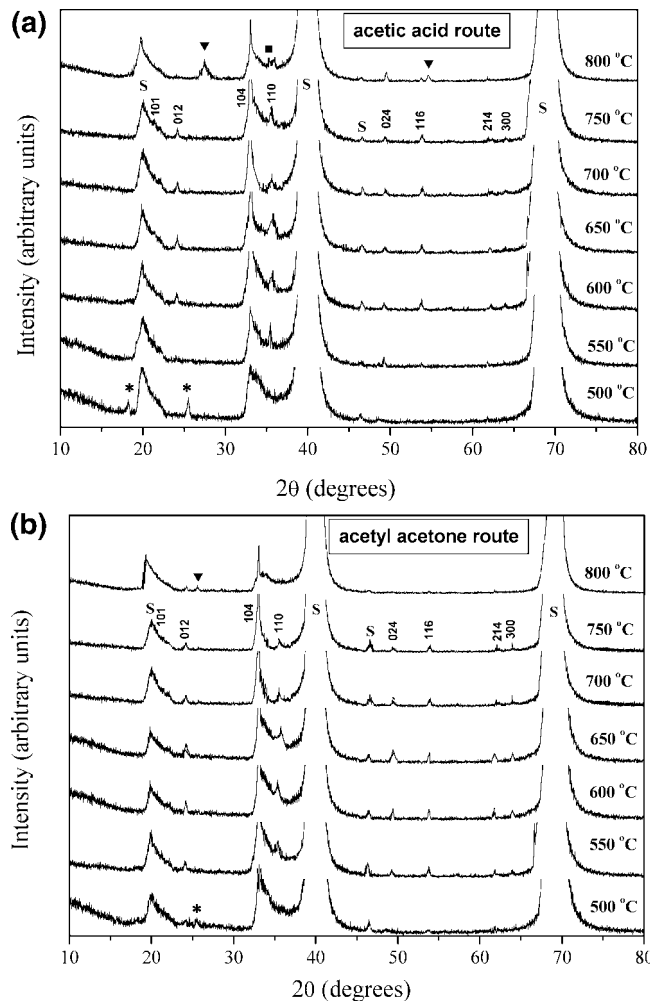


**Figure 5.** (a) X-ray diffraction patterns of the films derived from the acetic-acid-based route annealed at 500, 600, 650, 700, 750, and 800 °C for 1 h. (S represents  $\text{Pt/TiO}_2/\text{SiO}_2/(100)\text{Si}$  substrates, \* represents  $\text{MgTi}_2\text{O}_5$ ,  $\blacksquare$  represents  $\text{Mg}_2\text{TiO}_4$ , and  $\blacktriangledown$  represents rutile  $\text{TiO}_2$ ). (b) X-ray diffraction patterns of the films derived from acetyl acetone based route annealed at 500, 600, 650, 700, 750 and 800 °C for 1 h. (S represents  $\text{Pt/TiO}_2/\text{SiO}_2/(100)\text{Si}$  substrates, \* represents  $\text{MgTi}_2\text{O}_5$ , and  $\blacktriangledown$  represents rutile  $\text{TiO}_2$ ).

Panels a and b in Figure 5 depict the XRD pattern of thin films of  $\text{MgTiO}_3$  on  $\text{Pt/TiO}_2/\text{SiO}_2/(100)\text{Si}$  substrates, annealed at different temperatures. As evidenced by DTA/TG (panels a and b in Figure 3) and XRD analysis of dried gels (panels a and b in Figure 4), the crystallization of  $\text{MgTiO}_3$  is completed only at temperatures above 500 °C in both routes. When acetic-acid-derived films are annealed at 500 °C,  $\text{MgTiO}_3$  appears as the major phase but a trace amount of  $\text{MgTi}_2\text{O}_5$  is also visible in the XRD pattern (Figure 5a). In acetyl-acetone-derived film annealed at 500 °C, trace amounts of  $\text{MgTi}_2\text{O}_5$  become also noticeable, which vanishes on annealing at a higher temperature as shown in Figure 5b. It is evident from the XRD patterns that annealing the films at 650 °C yields the best crystallinity in acetic acid route, whereas 700 °C is the optimum temperature for the acetyl acetone route. Heat-treating the films at a temperature above 800 °C results in the dissociation of  $\text{MgTiO}_3$  into  $\text{Mg}_2\text{TiO}_4$  and  $\text{TiO}_2$  (rutile), as seen from panels a and b in Figure 5. The lower formation temperature of  $\text{MgTiO}_3$  in the acetic acid route is in agreement with the thermal analysis studies for which the onset of crystallization starts earlier (Figure 3a).

(16) Miao, Y.-M.; Zhang, Q.-L.; Yang, H.; Wang, H.-P. *Mater. Sci. Eng., B* **2006**, *128*, 103.



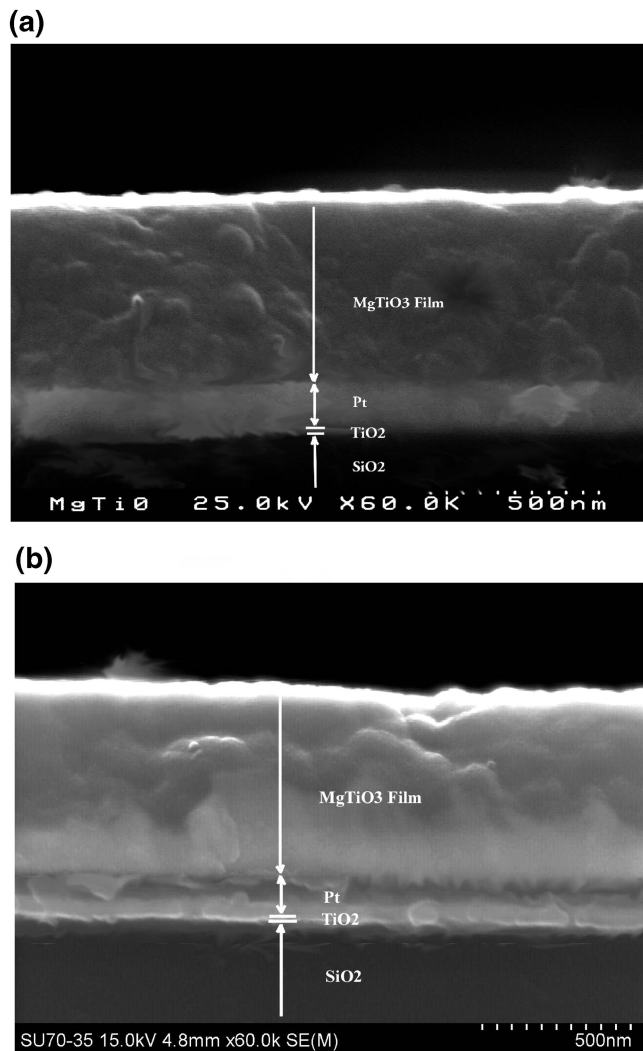


**Figure 6.** (a) SEM cross-section image of MgTiO<sub>3</sub> films derived from acetic-acid-based sols, annealed at 650 °C for 1 h. SEM cross-section image of MgTiO<sub>3</sub> films derived from acetyl acetone based sols, annealed at 650 °C for 1 h.

As discussed before, even though the acetic-acid-derived sol has slightly higher viscosity compared to the other one, it is not reflected as a noticeable difference in the thickness of their films. Images a and b in Figure 6 represent the SEM cross-sections of acetic-acid- and acetyl-acetone-derived films, respectively, annealed at 650 °C for 1 h. The thickness of both films was measured to be around 550 nm within the limits of experimental error. Although the cross-sectional SEM images a and b in Figure 6 look similar in densification, a clear morphological difference between the two microstructures could be detected with the help of AFM. The surface morphology of the two films annealed at 700 °C, shown in panels a and b in Figure 7, indicates different microstructure features. The topography of MgTiO<sub>3</sub> films delivered from acetic-acid-stabilized sols, showed relatively larger grains compared to that of films delivered from its acetyl acetone counterpart (see Figure 7a). Furthermore, amplitude image revealed that nanopores existed in these films, which were further confirmed by the phase image. The phase lag is very sensitive to variations in material properties such as adhesion and viscoelasticity. As pores entrapped air, which has different adhesion and viscoelasticity from those

of MgTiO<sub>3</sub> films, a clear contrast was shown in the phase image of this film derived from acetic acid based route (see Figure 7a). Topography of MgTiO<sub>3</sub> films delivered from acetyl acetone based sols showed fine grained films with average grain size of ~30 nm. It is also revealed from Figure 7b that these films have homogeneous and dense microstructures. Besides, the phase image showed clear grain features.

So, it is desired to inspect whether the observed differences in their microstructure is reflected in the dielectric properties of acetic-acid- and acetyl-acetone-derived films. The dielectric loss tangent of films annealed at various temperatures is presented in panels a and b in Figure 8. As expected, the loss tangent decreases when the frequency is increased from 100 Hz to 1 MHz. It is evident that the films prepared using acetic acid as the coordinating agent experience more loss compared to their acetyl acetone counterpart. The lowest loss in the acetic acid route is observed for films annealed at 650 °C ( $\tan \delta = 0.00728$  at 1 MHz), while for the acetyl-acetone-derived films is observed the ones annealed at 700 °C ( $\tan \delta = 0.00214$  at 1 MHz).

Panels a and b in Figure 9 represent the variation of dielectric constant and loss tangent of films fabricated using the two different routes, as a function of annealing temperature (500–800 °C). The dielectric constant of acetyl-acetone- and acetic-acid-based films annealed at 700 °C is 16. At annealing temperatures above 750 °C, the dielectric loss and dielectric constant increase in both cases (panels a and b in Figure 9). The dielectric loss of MgTiO<sub>3</sub> films prepared using the acetic-acid-based route is comparatively more sensitive to the annealing temperature than acetyl-acetone-based ones.

#### 4. Discussion

For the synthesis of ATiO<sub>3</sub> [A = alkaline earth ion] type compounds, the most commonly used sol–gel methodologies are<sup>14</sup> (a) conventional sol–gel processes that use 2-methoxyethanol as a reactant and solvent, (b) chelate processes that use modifying ligands such as acetic acid or acetyl acetone, and (c) metalloorganic decomposition (MOD) routes that use water-insensitive metal carboxylate compounds. Unlike conventional sol–gel routes, the chelate routes rely heavily on the molecular modification of the alkoxide compounds through reactions with coordinating agents, such as acetic acid or acetyl acetone. In such reactions involving titanium alkoxides, either acetic acid or acetyl acetone is added in order to control the hydrolysis of the titanium alkoxide.<sup>22</sup> Furthermore, it was shown that the incorporation of acetic acid or acetylacetone in the preparation of hybrid materials avoids the gelation of the reactive medium before the hydrolysis process and the titania precipitation.<sup>17</sup>

The esterification reactions of Ti(OBu)<sub>4</sub> with acetic acid have been reported in the literature.<sup>17,18</sup> When the molar ratio between the carboxylic acid and titanium butoxide is greater than 1, the formation of a carboxylate substituted oxo-clusters rather than carboxylate substituted titanium butoxide was

(17) Perrin, F. X.; Nguyen, V.; Vernet, J. L. *Polym. Int.* **2002**, *51*, 1013.

(18) Schubert, U. J. *Mater. Chem.* **2005**, *15*, 3701.

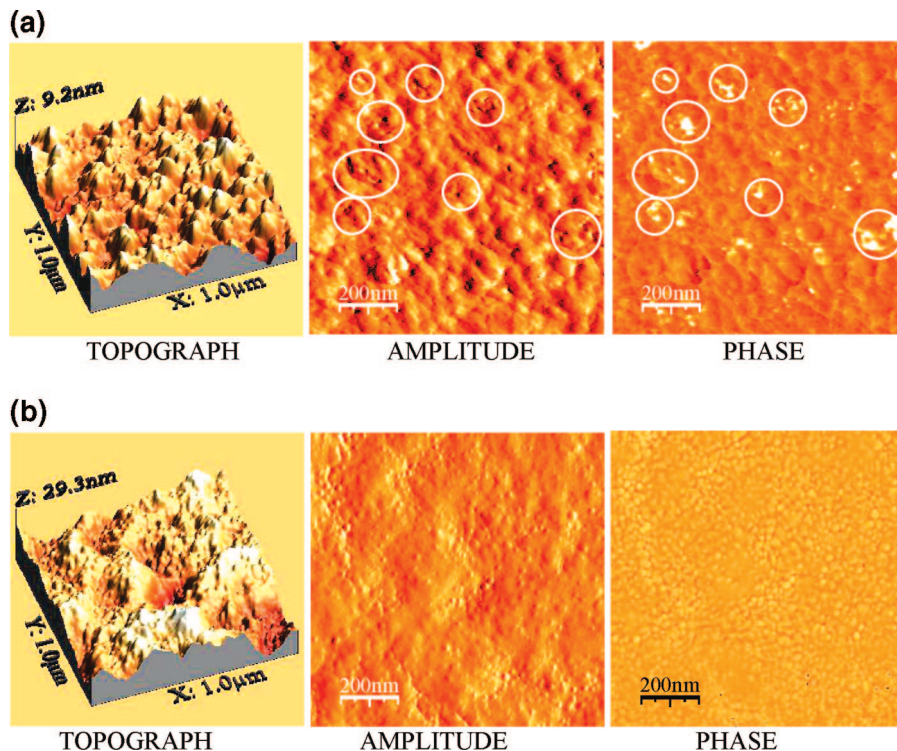


**Figure 7.** (a) AFM image of MgTiO<sub>3</sub> films derived from acetic-acid-based precursors and annealed at 700 °C (rms roughness = 1.55 nm). Major pores are encircled. AFM image of MgTiO<sub>3</sub> films derived from acetyl-acetone-based precursors and annealed at 700 °C, (rms roughness = 4.30 nm).

suggested. While the chemical modification of titanium alkoxides by  $\beta$ -diketones and the subsequent chelate formation, were also discussed elaborately in many reports.<sup>14</sup> In the present investigation, two sets of complex reaction mixtures are present, each containing (i) two metals with their own coordination chemistry, (ii) at least three potentially bidentate ligands (1,2 propanediol, acetic acid/acetyl acetone, nitrate), (iii) a mixture of alcohols, i.e., butanol, propanediol, ethanol (all can undergo exchange processes). This will result in complex reaction equilibria, and therefore it is not possible to easily assign spectroscopic data to a clearly defined precursor. Hence, a detailed spectroscopic characterization of the complex reaction mixtures derived from acetic acid and acetyl acetone based sol, is beyond the scope of the present investigation. However, though complicated, the 1,2 propanediol, nitrate, and ethanol are equally incorporated into the synthesis routes, the only difference raises from acetic-acid-modified titanium butoxide and acetylactone modified titanium butoxide. Hence for the reference purpose, the IR spectra of acetyl-acetone- and acetic-acid-based precursor species obtained in this study are provided in the Supporting Information. During film formation, the precursor species come together and begin to interact which is governed by size, shape, and reactivity of the species.<sup>14</sup> As a consequence, the thin film consolidation is different in both acetic-acid- and acetyl-acetone-based films. This fact is visible in their AFM images, as shown in panels a and b in Figure 7, where acetyl-acetone-based films show a better packing efficiency and homogeneity, compared to the more porous acetate delivered counterparts.

Concerning now the dielectric response of the films, it is then expected, based on sol stability and the consequent microstructures, that the dielectric properties of acetyl acetone

based films would be better compared to acetic acid based films. The dielectric loss of microwave materials (both films and ceramics) are highly sensitive to processing conditions, and the measured loss factor increases with the presence of porosity, microcracks, and impurity phases in the specimen. Indeed, in the present experiments, the dielectric loss of acetyl-acetone-based films is small, which is a consequence of the homogeneous morphology of the films, which are dense and crack free with a uniform grain size distribution (see Figure 7b). On the other hand there is a greater extent of nanoporosity visible only by AFM (encircled in Figure 7a) in acetic acid derived films, developed during the film's combustion and pyrolysis processes. Furthermore, it is worthwhile to note that the average grain size of acetate derived films ( $\sim 60$  nm) is larger than that of diketones based films ( $\sim 30$  nm). These observations of comparably high dielectric loss (see Figure 9a) in acetic-acid-based thin films, are consistent with the findings made by Alford et al.,<sup>19</sup> who after studying the dielectric loss of a variety of low-loss complex oxides concluded that dielectric loss of microwave dielectrics increases with increase in either porosity or grain size. Hence, it became evident that for developing high- $Q$  thin films, a dense and homogeneous microstructure is a primary prerequisite, which could be achieved by suitable modifications in the precursor chemistry.

In the present work, the lowest dielectric loss, 0.00214 at 1 MHz, is observed for MgTiO<sub>3</sub> films derived from acetyl acetone stabilized precursor, which were annealed at 700 °C. The dielectric loss of MgTiO<sub>3</sub> thin films reported in this investigation is understandably greater than that of bulk

(19) Alford, N.; Breeze, J.; Wang, X.; Penn, S. J.; Dalla, S.; Webb, S. J.; Ljepojevic, H.; Aupi, X. *J. Eur. Ceram. Soc.* **2001**, *21*, 2605.

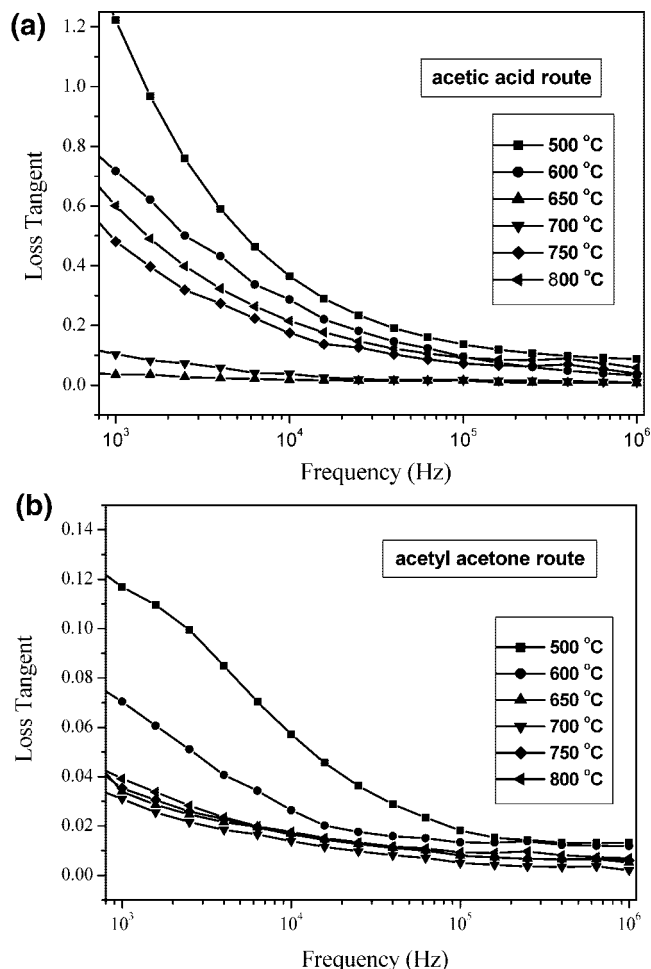


**Figure 8.** (a) Variation of the loss tangent of MgTiO<sub>3</sub> thin films prepared using acetic-acid-based sols and heated at different temperatures. (b) Variation of the loss tangent of MgTiO<sub>3</sub> thin films prepared using acetyl-acetone-based sols and heated at different temperatures.

ceramic samples ( $Q = 1/\tan \delta = 20\,000$  (at 8 GHz)). Even for one of the best known microwave dielectrics like Ba(Mg<sub>1/3</sub>Ta<sub>2/3</sub>)O<sub>3</sub>, the reported dielectric loss<sup>20</sup> for thin films ( $\tan \delta = 0.015$  at 1 MHz) is manifolds higher than that reported for ceramics. This is a common phenomenon seen in thin film dielectrics, which could be due to (i) strains developed at the film–substrate interface originating from the difference in thermal expansion between the film and the substrate<sup>21</sup> and (ii) imperfections or defects in the film caused by the synthesis process and by the substrate interface, as mentioned before. Moreover, the effects of series and parallel resistances due to parallel plate capacitor measurement configuration can also affect the measured dielectric loss values.<sup>22</sup> The intrinsic dissipation factor value is then expected to be even lower than 0.00214. Even though the measured loss factor for MgTiO<sub>3</sub> thin films prepared by sol gel in this work is considerably better than the values reported for MgTiO<sub>3</sub> thin films fabricated using rf-sputtering ( $\tan \delta = 0.041$  at 10 MHz).<sup>12</sup>

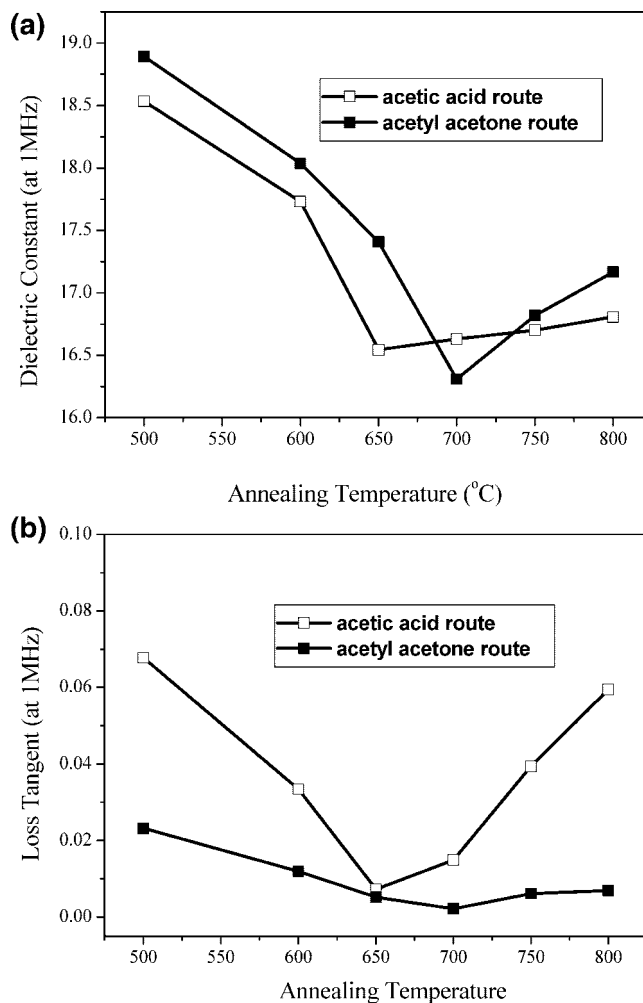


**Figure 9.** (a) Variation of dielectric constant (at 1 MHz) of MgTiO<sub>3</sub> thin films with different annealing temperatures. (b) Variation of loss tangent (at 1 MHz) of MgTiO<sub>3</sub> thin films with different annealing temperatures.

Finally, the films prepared from both routes showed, in general, high loss factor at low frequency. This might be related to the space charge polarization effects (because of the mobile charge carriers that may be present in the films), which are predominant at lower radio frequencies. As the applied frequency is increased, ionic polarization takes over. This mechanism is active in the 10<sup>3</sup> to 10<sup>6</sup> Hz range, which results in the lowering of dielectric loss near 1 MHz, as seen in this work. The dielectric constant and loss factor of the samples processed at low temperatures ( $\sim 500$  °C) are higher as seen in panels a and b in Figure 9 than those processed at high temperatures. At low processing temperatures, the films are less dense and both sets of samples contain trace amounts of MgTi<sub>2</sub>O<sub>5</sub>, which is also reported to have a high dielectric constant. Furthermore, annealing the films above optimum temperature can result in grain growth that can result in the increase in dielectric constant (see Figure 9a). In addition, the decomposition of MgTiO<sub>3</sub> (see panels a and b in Figure 4) at high temperatures ( $T > 750$  °C), also contributes significantly to the anomalous increase in dielectric loss factor and dielectric constant of the films annealed at high temperatures. These results clearly confirm the fact that a dense and homogeneous film microstructure is a basic prerequisite for good microwave dielectric properties.

(20) Chu, Y.-H.; Lin, S.-J.; Liu, K.-S.; Lin, I.-N. *Integr. Ferroelectr.* **2003**, *55*, 887.

(21) Horwitz, J. S.; Chang, W.; Kim, W.; Qadri, S. B.; Pond, J. M.; Kirchoefer, S. W.; Chrisey, D. B. *J. Electroceram.* **2000**, *4*, 357.

(22) Joshi, P. C.; Desu, S. B. *Appl. Phys. Lett.* **1998**, *73*, 1080.

## 5. Conclusions

The present paper outlined the fabrication of low-loss MgTiO<sub>3</sub> thin films at low temperature through a non-MOE sol gel route. Acetic acid and acetyl acetone were used as coordinating agents in the preparation of the sols. The sols using acetic-acid- and acetyl-acetone-based routes act differently in the thin film processing, and resulted in different chemical, microstructural, and dielectric properties. The crystallization of MgTiO<sub>3</sub> takes place below 520 °C when acetic acid was added as the stabilizer, whereas it occurred at a slightly higher temperature (540 °C) in its acetyl acetone counterpart. The acetyl-acetone-modified precursor is more stable against hydrolysis on aging, which also exhibited better packing efficiency on film consolidation. As a result of its dense and homogeneous microstructure, the dielectric loss

factor is lower ( $\tan \delta = 0.00214$  at 1 MHz) for MgTiO<sub>3</sub> films derived using acetyl acetone route, in comparison to acetic acid derived ones. This loss value is better than that of RF-sputtered MgTiO<sub>3</sub> thin films ( $\tan \delta = 0.041$  at 10 MHz) reported in literature.

**Acknowledgment.** The authors acknowledge FCT, FEDER, and the European Network of Excellence FAME under Contract FP6-500159-1. K.P.S. acknowledges FCT for financial support (SFRH/BPD/24538/2005).

**Supporting Information Available:** FT-IR spectra of sols derived from acetic-acid- and acetyl-acetone-based routes (PDF). This material is available free of charge via the Internet at <http://pubs.acs.org>.

CM703088M